

# Dark energy and matter interacting scenario can relieve $H_0$ and $S_8$ tensions

Li-Yang Gao,<sup>1,2,\*</sup> She-Sheng Xue,<sup>3,4,5,6,\*</sup> and Xin Zhang<sup>1,7,8,†</sup>

<sup>1</sup>Key Laboratory of Cosmology and Astrophysics (Liaoning Province) & Department of Physics, College of Sciences, Northeastern University, Shenyang 110819, China

<sup>2</sup>Kapteyn Astronomical Institute, University of Groningen, P.O. Box 800, 9700 AV Groningen, the Netherlands

<sup>3</sup>ICRANet, Piazzale della Repubblica, 10-65122, Pescara, Italy

<sup>4</sup>ICTP-AP, University of Chinese Academy of Sciences, Beijing, China

<sup>5</sup>Physics Department, Sapienza University of Rome, P.le A. Moro 5, 00185, Rome, Italy

<sup>6</sup>INFN, Sezione di Perugia, Via A. Pascoli, I-06123, Perugia, Italy

<sup>7</sup>Key Laboratory of Data Analytics and Optimization for Smart Industry (Ministry of Education), Northeastern University, Shenyang 110819, China

<sup>8</sup>National Frontiers Science Center for Industrial Intelligence and Systems Optimization, Northeastern University, Shenyang 110819, China

We consider a new cosmological model (named  $\tilde{\Lambda}$ CDM) in which the vacuum energy interacts with matter and radiation, and test this model using the current cosmological observations. Using the CMB+BAO+SN (CBS) data set to constrain the model, we find that the  $H_0$  and  $S_8$  tensions are relieved to  $2.87\sigma$  and  $2.77\sigma$ , respectively. However, in this case, the  $\tilde{\Lambda}$ CDM model is not favored by the data, compared with  $\Lambda$ CDM. We find that when the  $H_0$  and  $S_8$  data are added into the data combination, the situation is significantly improved. In the CBS+ $H_0$  case, we find that the model relieves the  $H_0$  tension to  $0.47\sigma$ , and in this case, the model is favored over  $\Lambda$ CDM. In the CBS+ $H_0$ + $S_8$  case, we get a synthetically best situation in which the  $H_0$  and  $S_8$  tensions are relieved to  $0.72\sigma$  and  $2.11\sigma$ , respectively. In this case, the model is most favored by the data. Therefore, such a cosmological model can greatly relieve the  $H_0$  tension, and at the same time, it can also effectively alleviate the  $S_8$  tension.

*Introduction.*—The discovery of the universe’s accelerated expansion in 1998 [1, 2] significantly invigorated interest in cosmology. Subsequent observations have continually supplied increasingly precise data, enhancing our understanding of this phenomenon. Key contributions include the cosmic microwave background (CMB) data from *Planck* 2018 [3] and the direct measurement of the Hubble constant,  $H_0$  [4]. The enhanced precision of these observational data has led to the emergence of the  $H_0$  and  $S_8$  tensions as prominent new challenges in the field.

The early-universe observation of *Planck* TT, TE, EE + lowE + lensing [3] combined with baryon acoustic oscillation (BAO) measurements from galaxy redshift surveys [5–7] gives a fit result of  $H_0 = 67.36 \pm 0.54 \text{ km s}^{-1}\text{Mpc}^{-1}$  for the  $\Lambda$ CDM model. The late-universe observation of the Cepheid-type Ia supernova (SN) distance ladder by SHOES [4] gives a result of  $H_0 = 73.04 \pm 1.04 \text{ km s}^{-1}\text{Mpc}^{-1}$ . Thus, the  $H_0$  tension has currently reached  $4.85\sigma$  [8–13]. In addition, the result of  $S_8 = 0.832 \pm 0.013$  obtained from *Planck* 2018 is also in a  $3.08\sigma$  tension with the result of  $S_8 = 0.766^{+0.020}_{-0.014}$  obtained from the combination of KiDS/Viking and SDSS cosmic shear data [14]. As the precision of the data increases, the  $H_0$  and  $S_8$  tensions become more pronounced. Consequently, one no longer believes that the issue is caused by the accuracy of the data but rather by issues with the measurements on one hand or by issues with the  $\Lambda$ CDM model on the other hand.

Numerous papers have attempted to examine the systematic flaws in both methodologies to address these ten-

sions (see, e.g., Refs. [15–21]), but no conclusive evidence has been found. As a result, new independent measurement techniques for late-universe observation have drawn attention, including, e.g., substitution of Mira variables [22] or red giants [23] for Cepheids in the Cepheid-SN distance ladder, observation of strong lensing time delays [24], water masers [25], surface brightness fluctuations [26], gravitational waves from neutron star mergers [27], use of different galaxies’ ages as cosmic clocks [28, 29], baryonic Tully-Fisher relation [30], and so on. Despite numerous new observations, the issue of  $H_0$  tension has not been resolved.

In this work, we assume that both early- and late-universe observations are credible and that the cosmological model has to be modified. The  $\Lambda$ CDM model has undergone numerous adaptations, which can be divided into two main groups: the dark energy model and the modified gravity model. Numerous dark energy models have been used to reduce  $H_0$  tension [31–53]. Others have explored modifications in gravitational theories, referred to as modified gravity (MG) models [54–58]. While these models partially mitigate the  $H_0$  tension, they often exacerbate the  $S_8$  tension [38].

Drawing upon the concepts of asymptotic safety [59] and particle production [60] in gravitational field theory, Ref. [61] introduced a  $\tilde{\Lambda}$ CDM model characterized by a dynamical vacuum energy component  $\tilde{\Lambda}$  that interacts with matter and radiation. The density of vacuum energy  $\rho_\Lambda(t) = \tilde{\Lambda}/(8\pi G)$  undergoes conversion to matter (radiation) and *vice versa*. The  $\tilde{\Lambda}$ CDM model has been

employed to investigate various cosmological phenomena, including inflation [62], reheating [63], and the evolution of standard cosmology from the end of reheating to the current era [64, 65]. Reference [66] presents a preliminary phenomenological study of the  $\tilde{\Lambda}$ CDM model, comparing with  $\Lambda$ CDM and other interacting dark energy models. Reference [40] presents the investigation of a simplified  $\tilde{\Lambda}$ CDM model, showing the possibility of greatly relieving the  $H_0$  tension. Here, we further study the  $H_0$  and  $S_8$  tensions and their correlations in the entire parameter space of the  $\tilde{\Lambda}$ CDM model.

To check if the model alleviates both the  $H_0$  and  $S_8$  tensions, we adopted the most commonly used data combination, CMB + BAO + SN (CBS). We also considered the  $H_0$  and  $S_8$  measurements as complements to CBS. Note that the redshifts of the galaxies used for measuring  $S_8$  are generally less than 1.5. We found that the model relieves the  $H_0$  tension to less than  $1\sigma$  and also simultaneously relieves the  $S_8$  tension, by simply using the CBS data. The least  $H_0$  and  $S_8$  tensions are achieved by using the CBS+ $H_0$  and CBS+ $H_0$ + $S_8$  data, respectively. Though the  $S_8$  tension is still slightly greater than  $2\sigma$ , we show that it is also definitely reduced when the  $H_0$  tension is reduced. This situation is difficult to appear in other cosmological models.

*Motivation and theoretical model.*— In the framework of the  $\tilde{\Lambda}$ CDM model in standard cosmology, particles are created in the neighbourhood of the Friedmann universe horizon. Such a dynamics is effectively described by the particle production rate  $\Gamma_m = -(\chi/4\pi)(\dot{H}/H^2)$  and the energy density  $\rho_m^H = 2\chi m^2 H^2$  of produced particles. Here,  $m$  stands for particles' mass, and  $\chi$  characterizes the width  $\chi/m$  of the particle-production layer on the horizon. The interplay between vacuum energy and matter (radiation) is delineated through the particle production rate  $\Gamma_m$  and density  $\rho_m^H$ , explicated in Refs. [63, 64] as

$$H^2 = \frac{8\pi G}{3}(\rho_m + \rho_r + \rho_\Lambda), \quad (1)$$

$$\dot{H} = -\frac{4\pi G}{3}(3\rho_m + 4\rho_r), \quad (2)$$

$$\dot{\rho}_m + 3H\rho_m = \Gamma_m(\rho_m^H - \rho_m - \rho_r), \quad (3)$$

$$\dot{\rho}_r + 4H\rho_r = \Gamma_m(\rho_r^H - \rho_m - \rho_r). \quad (4)$$

The matter density  $\rho_m$  is for non-relativistic particles, and the radiation density  $\rho_r$  for relativistic particles. Equations (1) and (2) are Friedmann equations for time-varying cosmological term  $\rho_\Lambda(t)$  and we have  $p_\Lambda = -\rho_\Lambda$ . Vacuum energy and matter (radiation) interact via the right-handed sides of energy conservation equations (3) and (4). With initial values at either the reheating end or today, four dynamic equations form a closed set giving unique solutions  $\rho_{m,r,\Lambda}$  and  $H$ .

The numerical solutions are too complex to proceed with data analysis. Nevertheless, the model accommo-

dates scaling solutions, consistent with the principles of asymptotic safety in gravitational theories [59, 61]. Namely, the  $\tilde{\Lambda}$ CDM quantities  $\rho_{m,r,\Lambda}$  receive scaling factor  $(1+z)^\delta$  (with  $|\delta| \ll 1$ ) corrections to  $\Lambda$ CDM counterparts when the redshift  $z$  becomes small (late times). Thus, we make ansatz solutions  $\rho_{m,r} \propto (1+z)^{3(1+w_{m,r})-\delta_G^{M,R}}$  deviating from the normal matter with  $w_m = 0$  and the normal radiation with  $w_r = 1/3$ , and  $\rho_\Lambda \propto (1+z)^{3(1+w_\Lambda)+\delta_\Lambda}$  deviating from the normal vacuum energy with  $w_\Lambda = -1$ .

Therefore, in late times, the  $\tilde{\Lambda}$ CDM model parameterizes the Friedman equation as

$$E^2(z) = \Omega_m(1+z)^{(3-\delta_G^M)} + \Omega_r(1+z)^{(4-\delta_G^R)} + \Omega_\Lambda(1+z)^{\delta_\Lambda}, \quad (5)$$

where  $E(z) = H(z)/H_0$ , and the three scaling indexes  $\delta_G^{M,R}$  and  $\delta_\Lambda$  are much smaller than unity. The generalized conservation law yields

$$(1+z) \frac{d}{dz} E^2(z) = 3\Omega_m(1+z)^{(3-\delta_G^M)} + 4\Omega_r(1+z)^{(4-\delta_G^R)}. \quad (6)$$

At the leading order of  $\delta_G^{M,R}$  and  $\delta_\Lambda$  and for low redshifts, we find the relation

$$\delta_\Lambda \approx (\Omega_m \delta_G^M + \Omega_r \delta_G^R) / \Omega_\Lambda. \quad (7)$$

Two independent parameters  $\delta_G^{M,R}$  can be constrained by observational data. Their negative (positive) values indicate the process of radiation and matter converting into dark energy (the inverse process). For comparative analysis, we also introduce the simplified  $\tilde{\Lambda}$ CDM model from our previous work [40], characterized by  $\delta_G \equiv \delta_G^M = \delta_G^R$  and  $\delta_\Lambda = \delta_G(\Omega_m + \Omega_r) / \Omega_\Lambda$ .

*Data and methodology.*— In this paper, we employ CMB, BAO, SN,  $H_0$ , and  $S_8$  data. For CMB data, we use *Planck* 2018 full-mission TT, TE, EE + lowE + lensing power spectrum [3]. For BAO data, we utilize five points from three observations (6dF Galaxy Survey, SDSS DR7 Main Galaxy Sample, and DR12 galaxy sample) [5–7]. For SN data, we use 1048 data points from the Pantheon compilation [67]. In addition, we also consider two Gaussian priors, i.e.,  $S_8 = 0.766_{-0.014}^{+0.020}$  [here  $S_8 \equiv \sigma_8(\Omega_m/0.3)^{0.5}$ ], which comes from the combination of the KiDS/Viking and SDSS data [14], and  $H_0 = 73.04 \pm 1.04 \text{ km s}^{-1} \text{ Mpc}^{-1}$ , which is determined from the distance ladder by the SH0ES team [4].

To conduct the Markov-chain Monte Carlo (MCMC) analysis, we use the `MontePython` code [68]. To assess how well the various models fit the data, we use the Akaike information criterion (AIC) [69–71],  $\text{AIC} \equiv \chi^2 + 2d$ , where  $d$  is the number of free parameters. We use  $\Delta\text{AIC} = \Delta\chi^2 + 2\Delta d$  to compare a model with  $\Lambda$ CDM.

*Results.*— To evaluate the  $\tilde{\Lambda}$ CDM model, we use the  $\Lambda$ CDM model as a reference model. First, we constrain the  $\Lambda$ CDM and  $\tilde{\Lambda}$ CDM models using the joint CBS data. The results are shown in Table I and Fig. 1.

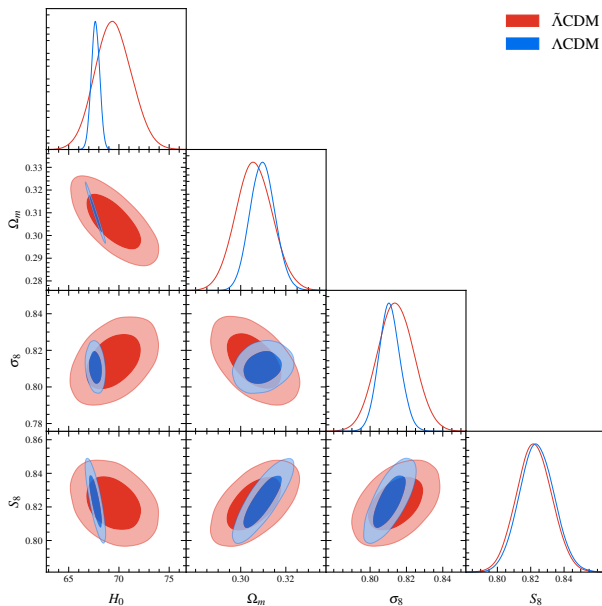


FIG. 1: Constraints (68.3% and 95.4% confidence level) on  $H_0$ ,  $\Omega_m$ ,  $\sigma_8$ , and  $S_8$  in the  $\Lambda$ CDM and  $\tilde{\Lambda}$ CDM models using the CBS data. Here,  $H_0$  is in units of  $\text{km s}^{-1} \text{Mpc}^{-1}$ .

Model	$\Lambda$ CDM	$\tilde{\Lambda}$ CDM
$\delta_G^M$	-	$-0.00052 \pm 0.00088$
$\delta_G^R$	-	$-0.0061 \pm 0.0059$
$\delta_\Lambda$	-	$-0.00022 \pm 0.00038$
$\Omega_m$	$0.3097 \pm 0.0055$	$0.3060 \pm 0.0081$
$H_0$ [ $\text{km s}^{-1} \text{Mpc}^{-1}$ ]	$67.66 \pm 0.41$	$69.5 \pm 1.8$
$\sigma_8$	$0.8107 \pm 0.0059$	$0.814 \pm 0.010$
$S_8$	$0.824 \pm 0.010$	$0.822 \pm 0.011$
$H_0$ tension	$4.81\sigma$	$2.87\sigma$
$S_8$ tension	$2.94\sigma$	$2.77\sigma$
$\chi_{\min}^2$	1907.55	1907.34
$\Delta\text{AIC}$	0	3.79

TABLE I: Constraint results of parameters in the  $\Lambda$ CDM and  $\tilde{\Lambda}$ CDM models with the CBS data. Here  $H_0$  is in units of  $\text{km s}^{-1} \text{Mpc}^{-1}$ .

In the  $\tilde{\Lambda}$ CDM model, we obtain the fit values of  $H_0 = 69.5 \pm 1.8 \text{ km s}^{-1} \text{Mpc}^{-1}$  and  $S_8 = 0.822 \pm 0.011$ , and thus now the  $H_0$  and  $S_8$  tensions are relieved to be at  $2.87\sigma$  and  $2.77\sigma$  levels, respectively. We find that in this case the  $H_0$  tension is greatly alleviated, and at the same time, the  $S_8$  tension is also slightly alleviated, which is difficult to be realized for other cosmological models.

While the  $\tilde{\Lambda}$ CDM model demonstrates potential in concurrently mitigating the  $H_0$  and  $S_8$  discrepancies, it leads to a larger AIC value compared to the  $\Lambda$ CDM model. This indicates that compared to  $\Lambda$ CDM, the  $\tilde{\Lambda}$ CDM model's capability in fitting observational data is somewhat weaker for the CBS case.

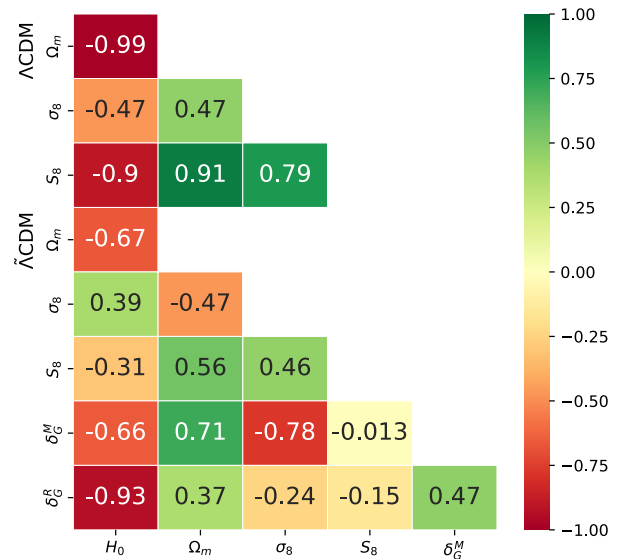


FIG. 2: Correlation coefficients between cosmological parameters in the  $\tilde{\Lambda}$ CDM and  $\Lambda$ CDM models using the CBS data.

To ascertain the  $\tilde{\Lambda}$ CDM model's potential in reducing both  $H_0$  and  $S_8$  tensions, we present the correlation coefficients between cosmological parameters of the  $\Lambda$ CDM and  $\tilde{\Lambda}$ CDM models in the CBS case in Fig. 2. Our findings reveal that within the  $\tilde{\Lambda}$ CDM model, the correlation coefficients of  $\delta_G^M$  and  $\delta_G^R$  with  $H_0$  are negative, and the current constraints give negative  $\delta_G^M$  and  $\delta_G^R$ . Consequently, the  $\tilde{\Lambda}$ CDM model significantly alleviates the  $H_0$  tension. Additionally, the extra free parameters exhibit weak correlations with  $S_8$ , suggesting that mitigating the  $S_8$  tension presents considerable challenges.

The evolution of  $\Omega_{m,r,\Lambda}$  with redshift  $z$  in the  $\tilde{\Lambda}$ CDM model exhibits similarities to the  $\Lambda$ CDM counterparts. To delineate the distinct characteristics between the  $\tilde{\Lambda}$ CDM and the  $\Lambda$ CDM models, we define the differences

$$\delta\Omega_{m,r,\Lambda}(z) = \Omega_{m,r,\Lambda}(z) - \Omega_{m,r,\Lambda}(z)|_{\Lambda\text{CDM}}. \quad (8)$$

Employing the constrained results from the CBS data set, as delineated in Table I and Fig. 1, we graphically represent the differences in Fig. 3. As shown in Fig. 3, the proportion of dark energy was nearly zero in the early universe, which is consistent with the  $\Lambda$ CDM model. However, in the late universe, when dark energy begins to dominate cosmic evolution, its proportion is somewhat larger than that predicted by the  $\Lambda$ CDM model. Correspondingly, the proportion of matter density in the late universe is slightly less than that in the standard model. This characteristic means that in this model, the accelerated expansion of the late universe begins earlier and is more intense. Consequently, the age of the universe is somewhat younger than that predicted by the standard model, resulting in a larger Hubble constant.

As shown in Table I and Fig. 1, the CBS data constrain

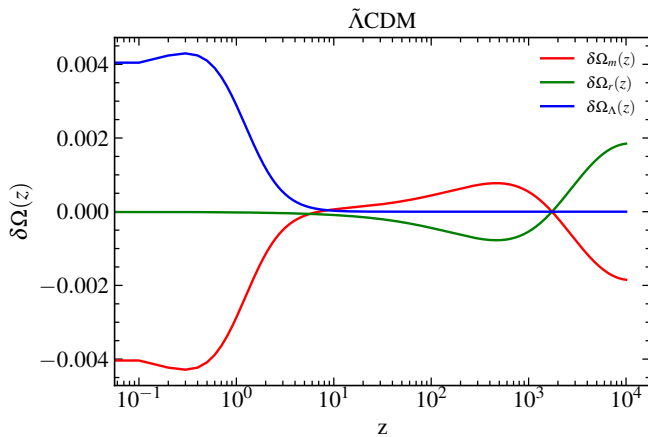


FIG. 3: The differences  $\delta\Omega_{m,r,\Lambda}(z)$  between the  $\tilde{\Lambda}$ CDM and  $\Lambda$ CDM models in the CBS case. Shown here is the best-fit result.

the  $\tilde{\Lambda}$ CDM  $H_0$  and  $\sigma_8$  ( $\Omega_m$ ), with the best-fit values larger (smaller) than the  $\Lambda$ CDM counterparts. Nonetheless, it is evident that the confidence ranges of these parameters are more broad in the  $\tilde{\Lambda}$ CDM model compared to the  $\Lambda$ CDM model. As a result, the  $H_0$  tension relieves to  $2.87\sigma$  in  $\tilde{\Lambda}$ CDM model.  $S_8 = \sigma_8(\Omega_m/0.3)^{0.5}$  depends on both  $\sigma_8$  and  $\Omega_m$ . The  $\tilde{\Lambda}$ CDM  $\Omega_m$  ( $\sigma_8$ ) best-fit value decreases (increases) and their spreading increase, resulting in decreasing the  $\tilde{\Lambda}$ CDM  $S_8$  tension to  $2.77\sigma$ , unlike increasing  $S_8$  tension in many other models. Consequently, the interaction dynamics between dark energy and matter, as illustrated in Fig. 3, are pivotal in substantially mitigating both  $H_0$  and  $S_8$  tensions.

At last, we constrain the  $\tilde{\Lambda}$ CDM model using the three data combinations, CBS+ $H_0$ , CBS+ $S_8$ , and CBS+ $H_0$ + $S_8$ . The constraint results are shown in Table II and Fig. 4. We also compute the AIC values for the  $\tilde{\Lambda}$ CDM model employing various data combinations to enable a systematic comparison between the  $\tilde{\Lambda}$ CDM and  $\Lambda$ CDM models across different data sets. In the previous case (the CBS case), though the  $H_0$  tension is greatly relieved, and the  $S_8$  tension is also slightly alleviated, the  $\tilde{\Lambda}$ CDM model is not favored by the CBS data because its  $\Delta\text{AIC}$  value is greater than 0 ( $\Delta\text{AIC} = 3.79$ ). However, when the  $H_0$  and  $S_8$  data are added into the data combination, we find that the situation is significantly improved both in relieving the tensions and fitting the observations.

In the CBS+ $H_0$  case, we have  $H_0 = 72.3 \pm 1.2$  km s $^{-1}$  Mpc $^{-1}$  and  $S_8 = 0.817 \pm 0.010$ . So in this case the  $H_0$  and  $S_8$  tensions are further relieved, and we can see that the  $H_0$  tension is greatly relieved to  $0.47\sigma$ . What's more, in this case  $\Delta\text{AIC} = -2.07$ , indicating that the  $\tilde{\Lambda}$ CDM model is favored by the data over  $\Lambda$ CDM. However, the  $\tilde{\Lambda}$ CDM model is not favored by the CBS+ $S_8$  data, in which though the  $S_8$  tension is slightly improved

(to  $2.43\sigma$ ), the  $H_0$  tension is slightly relieved (to  $1.96\sigma$ ), and the fit gives  $\Delta\text{AIC} = 5.02$ . Consequently, incorporating  $H_0$  and  $S_8$  priors into the data combination effectively mitigates the tensions. Therefore, employing the CBS+ $H_0$ + $S_8$  data set fosters an optimally synthesized scenario. In this scenario, we obtain  $H_0 = 71.9 \pm 1.2$  km s $^{-1}$  Mpc $^{-1}$  and  $S_8 = 0.8074 \pm 0.00998$ , consequently reducing the  $H_0$  and  $S_8$  tensions to  $0.72\sigma$  and  $2.11\sigma$ , respectively. Furthermore, under these conditions, the model exhibits the highest degree of concordance with the data, as indicated by  $\Delta\text{AIC} = -2.29$ .

We compare our findings with those derived from the simplified  $\tilde{\Lambda}$ CDM model [40], wherein it is postulated that  $\delta_G^M$  and  $\delta_G^R$  are identical in Eqs. (5) and (7), i.e.,  $\delta_G^M = \delta_G^R = \delta_G$ , and  $\delta_\Lambda = \delta_G(\Omega_m + \Omega_r)/\Omega_\Lambda$ . Employing the CBS data set, the  $H_0$  tension can be relieved to  $3.59\sigma$  (with the best fit  $H_0 = 67.71$  km s $^{-1}$  Mpc $^{-1}$ ) and in this case the  $S_8$  tension is exacerbated (with the best fit  $S_8 = 0.8252$ ). Additionally, within the simplified  $\tilde{\Lambda}$ CDM model constrained by the CBS +  $H_0$  data set, we have the best-fit values  $\sigma_8 = 0.8720$  and  $S_8 = 0.8310$ , and we can see that the  $\sigma_8$  and  $S_8$  tensions significantly increase while alleviating the  $H_0$  tension.

Additionally, we extend our comparison to the  $\Lambda(t)$ CDM model, an interacting vacuum energy model that posits an energy exchange between vacuum energy and cold dark matter as detailed by specific equations  $\dot{\rho}_\Lambda = \beta H \rho_c$  and  $\dot{\rho}_c + 3H \rho_c = -\beta H \rho_c$  (here the dimensionless parameter  $\beta$  describes the interaction strength). In Ref. [38], the same CBS+ $H_0$  data set is used to constrain  $\Lambda(t)$ CDM model to obtain  $H_0 = 69.36$  km s $^{-1}$  Mpc $^{-1}$  and  $\sigma_8 = 0.844$ . In contrast, the current findings, as illustrated in Table II, explicitly show that the  $\tilde{\Lambda}$ CDM model exhibits distinct advantages relative to the  $\Lambda(t)$ CDM model.

*Conclusion.*—In this work, we proposed a new cosmological model in which the vacuum energy interacts with matter and radiation, which is considered to originate from the asymptotic safety and particle production of gravitational quantum field theory. We tested this model using the current cosmological observations and discussed its capability of relieving the  $H_0$  and  $S_8$  tensions.

To elucidate the mechanisms by which the  $\tilde{\Lambda}$ CDM model ameliorates tensions, we analyzed the differences  $\delta\Omega_{m,r,\Lambda}(z)$  between the  $\tilde{\Lambda}$ CDM and  $\Lambda$ CDM models. The alleviation of the  $H_0$  tension is attributed to the  $\tilde{\Lambda}$ CDM model's enhanced dark energy proportion and reduced matter fraction at low redshifts relative to the  $\Lambda$ CDM model, stemming from the conversion of matter into dark energy. The findings of  $\delta_G^{M,R} < 0$  and  $\delta_\Lambda < 0$  corroborate the  $\tilde{\Lambda}$ CDM hypothesis in which in the late universe radiation and matter decay into dark energy [64, 65].

We find that this cosmological model can significantly relieve the  $H_0$  tension, and at the same time, it can also

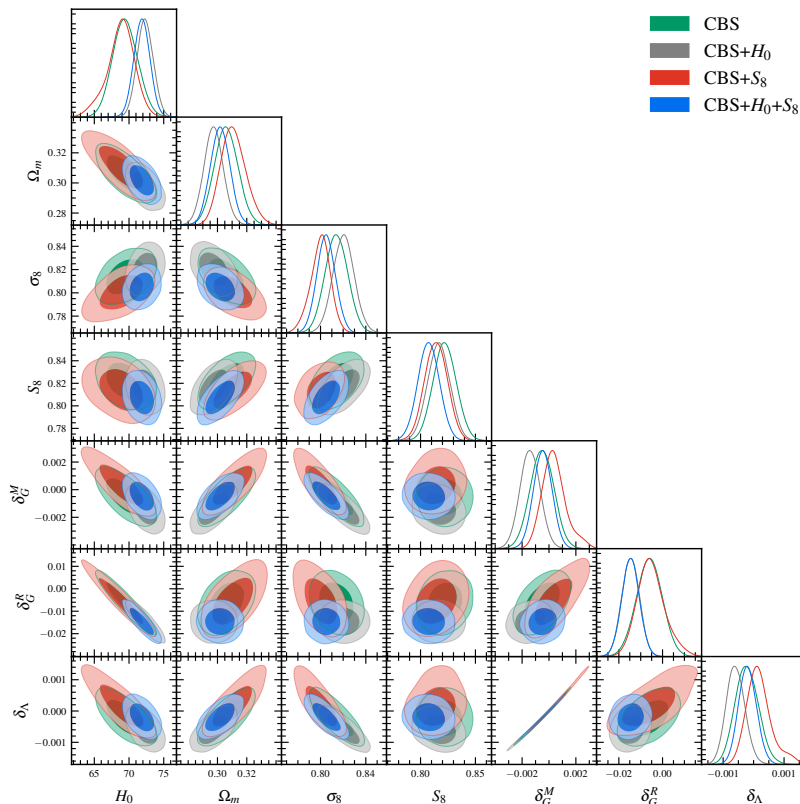


FIG. 4: Constraints (68.3% and 95.4% confidence level) on the  $\tilde{\Lambda}$ CDM model using CBS, CBS+ $H_0$ , CBS+ $S_8$ , and CBS+ $H_0$ + $S_8$  data.  $H_0$  is in units of  $\text{km s}^{-1} \text{Mpc}^{-1}$ .

Data	CBS+ $H_0$	CBS+ $S_8$	CBS+ $H_0$ + $S_8$
$\delta_G^M$	$-0.00140 \pm 0.00075$	$0.00038^{+0.00072}_{-0.00098}$	$-0.00046 \pm 0.00069$
$\delta_G^R$	$-0.0146 \pm 0.0040$	$-0.0053^{+0.0055}_{-0.0068}$	$-0.0147 \pm 0.0040$
$\delta_\Lambda$	$-0.00059 \pm 0.00030$	$0.00018^{+0.00031}_{-0.00046}$	$-0.00020 \pm 0.00029$
$\Omega_m$	$0.2974 \pm 0.0066$	$0.3108^{+0.0077}_{-0.0091}$	$0.3018 \pm 0.0066$
$H_0$	$72.3 \pm 1.2$	$68.8^{+2.1}_{-1.7}$	$71.9 \pm 1.2$
$\sigma_8$	$0.8203 \pm 0.0095$	$0.8000^{+0.0093}_{-0.0079}$	$0.8050 \pm 0.0081$
$S_8$	$0.817 \pm 0.010$	$0.814 \pm 0.010$	$0.8074 \pm 0.0098$
$H_0$ tension	$0.47\sigma$	$1.96\sigma$	$0.72\sigma$
$S_8$ tension	$2.59\sigma$	$2.43\sigma$	$2.11\sigma$
$\chi^2_{\min}$	1909.53	1912.46	1914.76
$\Delta\text{AIC}$	-2.07	5.02	-2.29

TABLE II: Constraint results of parameters in the  $\tilde{\Lambda}$ CDM model with CBS+ $H_0$ , CBS+ $S_8$ , and CBS+ $H_0$ + $S_8$  data.

slightly reduce the  $S_8$  tension, which cannot be easily observed in other cosmological models. When using the CBS data to constrain the model, we find that the  $H_0$  tension is relieved to  $2.87\sigma$ , and meanwhile, the  $S_8$  tension is also improved to  $2.77\sigma$ . But in this case, the  $S_8$  tension is only slightly reduced, and actually, the model is not favored by the CBS data (since  $\Delta\text{AIC} = 3.79$ ).

When the  $H_0$  and  $S_8$  data are added into the data combination, the situation is significantly improved. In the

CBS+ $H_0$  case, we obtain the result of  $H_0 = 72.3 \pm 1.2 \text{ km s}^{-1} \text{Mpc}^{-1}$ , indicating that the  $H_0$  tension is relieved to  $0.47\sigma$ , and in this case the model is favored over  $\Lambda$ CDM ( $\Delta\text{AIC} = -2.07$ ). In the CBS+ $H_0$ + $S_8$  case, we get a synthetically best situation, in which we have  $H_0 = 71.9 \pm 1.2 \text{ km s}^{-1} \text{Mpc}^{-1}$  and  $S_8 = 0.8074 \pm 0.0098$ , thus the  $H_0$  and  $S_8$  tensions are relieved to  $0.72\sigma$  and  $2.11\sigma$ , respectively. In this case, the model is most favored by the data ( $\Delta\text{AIC} = -2.29$ ).

Therefore, we find that such a cosmological model can greatly relieve the  $H_0$  tension, and at the same time, it can also alleviate the  $S_8$  tension.

Undoubtedly, this model requires further in-depth research in many aspects. Such an interaction between vacuum energy and matter is likely to bring many additional observational effects. For example, we are not sure whether this model will lead to a significant integrated Sachs-Wolfe effect. Further research on this issue requires further related theoretical study and analysis using full CMB angular power spectrum data. Another example is that this additional interaction may also lead to modifications in the middle-scale clustering patterns in large-scale structures, which will potentially affect the clustering strength at various scales. Therefore, such modifications may also affect the mass function and profile of dark matter halos, the statistical properties of galaxy clusters, the alignments of galaxies, the structure of the cosmic web, and so on. The study of these effects is a complicated issue and requires the use of N-body simulations, and also relies on assumptions about the nature of dark matter (such as cold dark matter or fuzzy dark matter). All these aspects deserve further in-depth discussion.

This work was supported by the National SKA Program of China (Grants Nos. 2022SKA0110200 and 2022SKA0110203) and the National Natural Science Foundation of China (Grants Nos. 11975072, 11875102, and 11835009).

---

\* These authors contributed equally to this paper.

† Corresponding author.

zhangxin@mail.neu.edu.cn

- [1] A. G. Riess *et al.* (Supernova Search Team), *Astron. J.* **116**, 1009 (1998), [arXiv:astro-ph/9805201](#) .
- [2] S. Perlmutter *et al.* (Supernova Cosmology Project), *Astrophys. J.* **517**, 565 (1999), [arXiv:astro-ph/9812133](#) .
- [3] N. Aghanim *et al.* (Planck), *Astron. Astrophys.* **641**, A6 (2020), [Erratum: *Astron. Astrophys.* 652, C4 (2021)], [arXiv:1807.06209 \[astro-ph.CO\]](#) .
- [4] A. G. Riess *et al.*, *Astrophys. J. Lett.* **934**, L7 (2022), [arXiv:2112.04510 \[astro-ph.CO\]](#) .
- [5] F. Beutler, C. Blake, M. Colless, D. H. Jones, L. Staveley-Smith, L. Campbell, Q. Parker, W. Saunders, and F. Watson, *Mon. Not. Roy. Astron. Soc.* **416**, 3017 (2011), [arXiv:1106.3366 \[astro-ph.CO\]](#) .
- [6] A. J. Ross, L. Samushia, C. Howlett, W. J. Percival, A. Burden, and M. Manera, *Mon. Not. Roy. Astron. Soc.* **449**, 835 (2015), [arXiv:1409.3242 \[astro-ph.CO\]](#) .
- [7] S. Alam *et al.* (BOSS), *Mon. Not. Roy. Astron. Soc.* **470**, 2617 (2017), [arXiv:1607.03155 \[astro-ph.CO\]](#) .
- [8] E. Di Valentino, O. Mena, S. Pan, L. Visinelli, W. Yang, A. Melchiorri, D. F. Mota, A. G. Riess, and J. Silk, *Class. Quant. Grav.* **38**, 153001 (2021), [arXiv:2103.01183 \[astro-ph.CO\]](#) .
- [9] L. Verde, T. Treu, and A. G. Riess, *Nature Astron.* **3**, 891 (2019), [arXiv:1907.10625 \[astro-ph.CO\]](#) .
- [10] E. Di Valentino, *Nature Astron.* **1**, 569 (2017), [arXiv:1709.04046 \[physics.pop-ph\]](#) .
- [11] E. Di Valentino *et al.*, *Astropart. Phys.* **131**, 102605 (2021), [arXiv:2008.11284 \[astro-ph.CO\]](#) .
- [12] W. L. Freedman, *Nature Astron.* **1**, 0121 (2017), [arXiv:1706.02739 \[astro-ph.CO\]](#) .
- [13] A. G. Riess, *Nature Rev. Phys.* **2**, 10 (2019), [arXiv:2001.03624 \[astro-ph.CO\]](#) .
- [14] C. Heymans *et al.*, *Astron. Astrophys.* **646**, A140 (2021), [arXiv:2007.15632 \[astro-ph.CO\]](#) .
- [15] D. N. Spergel, R. Flauger, and R. Hlozek, *Phys. Rev. D* **91**, 023518 (2015), [arXiv:1312.3313 \[astro-ph.CO\]](#) .
- [16] G. E. Addison, Y. Huang, D. J. Watts, C. L. Bennett, M. Halpern, G. Hinshaw, and J. L. Weiland, *Astrophys. J.* **818**, 132 (2016), [arXiv:1511.00055 \[astro-ph.CO\]](#) .
- [17] N. Aghanim *et al.* (Planck), *Astron. Astrophys.* **607**, A95 (2017), [arXiv:1608.02487 \[astro-ph.CO\]](#) .
- [18] G. Efstathiou, *Mon. Not. Roy. Astron. Soc.* **440**, 1138 (2014), [arXiv:1311.3461 \[astro-ph.CO\]](#) .
- [19] W. Cardona, M. Kunz, and V. Pettorino, *JCAP* **03**, 056 (2017), [arXiv:1611.06088 \[astro-ph.CO\]](#) .
- [20] B. R. Zhang, M. J. Childress, T. M. Davis, N. V. Karpenka, C. Lidman, B. P. Schmidt, and M. Smith, *Mon. Not. Roy. Astron. Soc.* **471**, 2254 (2017), [arXiv:1706.07573 \[astro-ph.CO\]](#) .
- [21] B. Follin and L. Knox, *Mon. Not. Roy. Astron. Soc.* **477**, 4534 (2018), [arXiv:1707.01175 \[astro-ph.CO\]](#) .
- [22] C. D. Huang, A. G. Riess, W. Yuan, L. M. Macri, N. L. Zakamska, S. Casertano, P. A. Whitelock, S. L. Hoffmann, A. V. Filippenko, and D. Scolnic, *Astrophys. J.* (2019), 10.3847/1538-4357/ab5dbd, [arXiv:1908.10883 \[astro-ph.CO\]](#) .
- [23] W. Yuan, A. G. Riess, L. M. Macri, S. Casertano, and D. Scolnic, *Astrophys. J.* **886**, 61 (2019), [arXiv:1908.00993 \[astro-ph.GA\]](#) .
- [24] K. C. Wong *et al.*, *Mon. Not. Roy. Astron. Soc.* **498**, 1420 (2020), [arXiv:1907.04869 \[astro-ph.CO\]](#) .
- [25] D. W. Pesce *et al.*, *Astrophys. J. Lett.* **891**, L1 (2020), [arXiv:2001.09213 \[astro-ph.CO\]](#) .
- [26] J. B. Jensen, J. L. Tonry, and G. A. Luppino, *Astrophys. J.* **505**, 111 (1998), [arXiv:astro-ph/9804169](#) .
- [27] B. P. Abbott *et al.* (LIGO Scientific, Virgo, 1M2H, Dark Energy Camera GW-E, DES, DLT40, Las Cumbres Observatory, VINROUGE, MASTER), *Nature* **551**, 85 (2017), [arXiv:1710.05835 \[astro-ph.CO\]](#) .
- [28] R. Jimenez and A. Loeb, *Astrophys. J.* **573**, 37 (2002), [arXiv:astro-ph/0106145](#) .
- [29] M. Moresco, L. Pozzetti, A. Cimatti, R. Jimenez, C. Maraston, L. Verde, D. Thomas, A. Citro, R. Tojeiro, and D. Wilkinson, *JCAP* **05**, 014 (2016), [arXiv:1601.01701 \[astro-ph.CO\]](#) .
- [30] J. Schombert, S. McGaugh, and F. Lelli, *Astron. J.* **160**, 71 (2020), [arXiv:2006.08615 \[astro-ph.CO\]](#) .
- [31] E. V. Linder, *Phys. Rev. Lett.* **90**, 091301 (2003), [arXiv:astro-ph/0208512](#) .
- [32] J. Grande, J. Sola, and H. Stefancic, *JCAP* **08**, 011 (2006), [arXiv:gr-qc/0604057](#) .
- [33] K. Dutta, Ruchika, A. Roy, A. A. Sen, and M. M. Sheikh-Jabbari, *Gen. Rel. Grav.* **52**, 15 (2020), [arXiv:1808.06623 \[astro-ph.CO\]](#) .
- [34] O. Akarsu, J. D. Barrow, L. A. Escamilla, and J. A. Vazquez, *Phys. Rev. D* **101**, 063528 (2020), [arXiv:1912.08751 \[astro-ph.CO\]](#) .

- [35] G. Ye and Y.-S. Piao, *Phys. Rev. D* **101**, 083507 (2020), [arXiv:2001.02451 \[astro-ph.CO\]](#) .
- [36] J. A. Vazquez, S. Hee, M. P. Hobson, A. N. Lasenby, M. Ibison, and M. Bridges, *JCAP* **07**, 062 (2018), [arXiv:1208.2542 \[astro-ph.CO\]](#) .
- [37] R. Calderón, R. Gannouji, B. L’Huillier, and D. Polarski, *Phys. Rev. D* **103**, 023526 (2021), [arXiv:2008.10237 \[astro-ph.CO\]](#) .
- [38] R.-Y. Guo, J.-F. Zhang, and X. Zhang, *JCAP* **02**, 054 (2019), [arXiv:1809.02340 \[astro-ph.CO\]](#) .
- [39] R.-Y. Guo, L. Feng, T.-Y. Yao, and X.-Y. Chen, *JCAP* **12**, 036 (2021), [arXiv:2110.02536 \[gr-qc\]](#) .
- [40] L.-Y. Gao, Z.-W. Zhao, S.-S. Xue, and X. Zhang, *JCAP* **07**, 005 (2021), [arXiv:2101.10714 \[astro-ph.CO\]](#) .
- [41] M.-M. Zhao, D.-Z. He, J.-F. Zhang, and X. Zhang, *Phys. Rev. D* **96**, 043520 (2017), [arXiv:1703.08456 \[astro-ph.CO\]](#) .
- [42] X. Zhang, *Phys. Rev. D* **93**, 083011 (2016), [arXiv:1511.02651 \[astro-ph.CO\]](#) .
- [43] J.-F. Zhang, Y.-H. Li, and X. Zhang, *Phys. Lett. B* **740**, 359 (2015), [arXiv:1403.7028 \[astro-ph.CO\]](#) .
- [44] L. Feng, D.-Z. He, H.-L. Li, J.-F. Zhang, and X. Zhang, *Sci. China Phys. Mech. Astron.* **63**, 290404 (2020), [arXiv:1910.03872 \[astro-ph.CO\]](#) .
- [45] M. Li, X.-D. Li, Y.-Z. Ma, X. Zhang, and Z. Zhang, *JCAP* **09**, 021 (2013), [arXiv:1305.5302 \[astro-ph.CO\]](#) .
- [46] J. C. Hill, E. McDonough, M. W. Toomey, and S. Alexander, *Phys. Rev. D* **102**, 043507 (2020), [arXiv:2003.07355 \[astro-ph.CO\]](#) .
- [47] M. M. Ivanov, E. McDonough, J. C. Hill, M. Simonović, M. W. Toomey, S. Alexander, and M. Zaldarriaga, *Phys. Rev. D* **102**, 103502 (2020), [arXiv:2006.11235 \[astro-ph.CO\]](#) .
- [48] T. L. Smith, V. Poulin, J. L. Bernal, K. K. Boddy, M. Kamionkowski, and R. Murgia, *Phys. Rev. D* **103**, 123542 (2021), [arXiv:2009.10740 \[astro-ph.CO\]](#) .
- [49] T. L. Smith, V. Poulin, and M. A. Amin, *Phys. Rev. D* **101**, 063523 (2020), [arXiv:1908.06995 \[astro-ph.CO\]](#) .
- [50] P. Agrawal, F.-Y. Cyr-Racine, D. Pinner, and L. Randall, *arXiv e-prints* (2019), [arXiv:1904.01016 \[astro-ph.CO\]](#) .
- [51] S. Alexander and E. McDonough, *Phys. Lett. B* **797**, 134830 (2019), [arXiv:1904.08912 \[astro-ph.CO\]](#) .
- [52] F. Niedermann and M. S. Sloth, *Phys. Rev. D* **103**, L041303 (2021), [arXiv:1910.10739 \[astro-ph.CO\]](#) .
- [53] N. Kaloper, *Int. J. Mod. Phys. D* **28**, 1944017 (2019), [arXiv:1903.11676 \[hep-th\]](#) .
- [54] B. Boisseau, H. Giacomini, D. Polarski, and A. A. Starobinsky, *JCAP* **07**, 002 (2015), [arXiv:1504.07927 \[gr-qc\]](#) .
- [55] M. Braglia, M. Ballardini, W. T. Emond, F. Finelli, A. E. Gumrukcuoglu, K. Koyama, and D. Paoletti, *Phys. Rev. D* **102**, 023529 (2020), [arXiv:2004.11161 \[astro-ph.CO\]](#) .
- [56] G. Ballesteros, A. Notari, and F. Rompineve, *JCAP* **11**, 024 (2020), [arXiv:2004.05049 \[astro-ph.CO\]](#) .
- [57] M. Ballardini, M. Braglia, F. Finelli, D. Paoletti, A. A. Starobinsky, and C. Umiltà, *JCAP* **10**, 044 (2020), [arXiv:2004.14349 \[astro-ph.CO\]](#) .
- [58] M. Zumalacarregui, *Phys. Rev. D* **102**, 023523 (2020), [arXiv:2003.06396 \[astro-ph.CO\]](#) .
- [59] S. Weinberg, *Phys. Rev. D* **81**, 083535 (2010), [arXiv:0911.3165 \[hep-th\]](#) .
- [60] L. Parker and S. A. Fulling, *Phys. Rev. D* **7**, 2357 (1973).
- [61] S.-S. Xue, *Nucl. Phys. B* **897**, 326 (2015), [arXiv:1410.6152 \[gr-qc\]](#) .
- [62] S.-S. Xue, *Eur. Phys. J. C* **83**, 36 (2023), [arXiv:2112.09661 \[gr-qc\]](#) .
- [63] S.-S. Xue, *Eur. Phys. J. C* **83**, 355 (2023), [arXiv:2006.15622 \[gr-qc\]](#) .
- [64] S.-S. Xue, *arXiv e-prints* (2023), [arXiv:2309.15488 \[gr-qc\]](#) .
- [65] S.-S. Xue, *arXiv e-prints* (2022), [arXiv:2203.11918 \[gr-qc\]](#) .
- [66] D. Bégulé, C. Stahl, and S.-S. Xue, *Nucl. Phys. B* **940**, 312 (2019), [arXiv:1702.03185 \[astro-ph.CO\]](#) .
- [67] D. M. Scolnic *et al.* (Pan-STARRS1), *Astrophys. J.* **859**, 101 (2018), [arXiv:1710.00845 \[astro-ph.CO\]](#) .
- [68] B. Audren, J. Lesgourgues, K. Benabed, and S. Prunet, *Journal of Cosmology and Astroparticle Physics* **02**, 001 (2012).
- [69] M. Szydlowski, A. Krawiec, A. Kurek, and M. Kamionka, *Eur. Phys. J. C* **75**, 5 (2015), [arXiv:0801.0638 \[astro-ph\]](#) .
- [70] D. Huterer, D. Shafer, D. Scolnic, and F. Schmidt, *JCAP* **05**, 015 (2017), [arXiv:1611.09862 \[astro-ph.CO\]](#) .
- [71] S. del Campo, J. C. Fabris, R. Herrera, and W. Zimdahl, *Phys. Rev. D* **83**, 123006 (2011), [arXiv:1103.3441 \[astro-ph.CO\]](#) .